Ultrasound in Med. & Biol., Vol. 30, No. 2, pp. 147–154, 2004

0301-5629/04/$–see front matter

ELSEVIER

doi:10.1016/j.ultrasmedbio.2003.10.014

● *Original Contribution*

SIMULTANEOUS ASSESSMENT OF DIAMETER AND PRESSURE WAVEFORMS IN THE CAROTID ARTERY

JAN M. MEINDERS* and ARNOLD P.G. HOEKS
Department of Biophysics, Cardiovascular Research Institute Maastricht, Maastricht University, Maastricht, Netherlands

(*Received* 9 *June* 2003; *revised* 22 *September* 2003; *in final form* 14 *October* 2003)

Abstract—Simultaneous assessment of diameter and pressure waveforms allows the calculation of the incremental compliance, distensibility, pulse wave velocity and elastic modulus as function of the distending pressure. However, the waveforms must be obtained at the same position and acquired and processed with the same filter characteristics to circumvent possible temporal and spatial changes in amplitude and phase. In this paper, arterial diameter waveforms are assessed by means of ultrasound (US) and converted to pressure using an empirically derived exponential relationship between pressure and arterial cross-section. The derived pressure waveform is calibrated to brachial end diastolic and mean arterial pressure by iteratively changing the wall rigidity coefficient (*i.e.*, the exponential power). Because pressure is derived directly from arterial cross-section, no phase delay is introduced due to spatial separation or different filter characteristics. The method was evaluated for the left common carotid artery of 51 healthy subjects ranging in age from 22 to 75 years old. In healthy subjects, the carotid pulse pressure is 29% lower than the brachial pulse pressure. Continuous assessment of arterial properties confirms that pulse-wave velocity and incremental elastic modulus increase, whereas distensibility and compliance decrease, as function of increasing distending blood pressure. (E-mail: j.meinders@bf.unimaas.nl)

Key Words: **Pressure waveform, Diameter waveform, Arterial stiffness, Wall rigidity, Carotid pulse pressure, Distensibility, Compliance, Elastic modulus, Pulse wave velocity.**

INTRODUCTION

Absence of possibilities to assess pressure at specific sites in the arterial tree complicates evaluation of arterial wall characteristics and hemodynamics. For instance, to determine the local elastic modulus of an arterial wall, the local pressure waveform has to be assessed simultaneously with the diameter waveform and vessel wall thickness. Diameter waveforms and vessel wall thickness can be obtained accurately using ultrasound (US) (Hoeks et al. 1990, 1997). Several methods have been proposed to assess local pressure waveforms; however, most of them suffer from one or more drawbacks. The invasive nature of a pressure catheter inserted in the artery under investigation probably influences local conditions of flow and geometry and is, also, not very suitable for routine examination. Use of pressure waveforms assessed at other sites in the arterial tree is questionable because the pressure waveform changes with the location in the arterial tree (Nichols and O'Rourke 1998) and introduces a phase delay between diameter and pressure, resulting in erroneous conclusions about the viscoelastic properties of the arterial wall (Hoeks et al. 2000). To reduce the site-dependence of pressure, a generalized transfer function may be used. Although the generalized transfer function has proven to be useful (O'Rourke 1999; Millasseau et al. 2000), it is an average over many subjects; thus, specific individual information may be lost (Segers et al. 2000). Furthermore, nonlinear propagation of the pulse-wave velocity (PWV) as function of the distending pressure is neglected and the phase delay between diameter and pressure still remains.

Applanation tonometry allows noninvasive assessment of the local pressure waveform. Good results are obtained after calibration of the applanation pressure waveform to the mean arterial blood pressure and diastolic blood pressure, which are assumed to be the same throughout the major arteries (Kelly and Fitchett 1992; van Bortel et al. 2001). However, simultaneous assessment of pressure and diameter (lumen area waveform) is difficult, not only due to the physical dimensions of both

Address correspondence to: J. M. Meinders, Ph.D., Department of Biophysics, CARIM, Maastricht University, P.O. Box 616, Maastricht 6200 MD Netherlands. E-mail: j.meinders@bf.unimaas.nl

transducers but, also, due to the different signal processing procedures resulting in erroneous phase delays and wrong conclusions about (viscoelastic) arterial properties (Hoeks et al. 2000). Furthermore, applanation tonometry cannot be applied to obese subjects or some arterial sites because it requires a stiff or bony background structure to flatten the artery wall, and a lean skin to avoid cushioning of the pressure pulse.

Deriving the blood pressure waveform from the diameter waveform avoids the use of generalized conversion factors and solves, also, the problem of modified phase delays. To obtain the pressure waveform, the minimum (d_d) and mean arterial diameter ($\bar{d}$) are calibrated to the end diastolic (p_d) and mean arterial pressure ($\bar{p}$). Subsequently, peak systolic pressure (p_s) is derived from the peak systolic diameter (d_s) (*i.e.*, $p_s = d_s^*(\bar{p} - p_d)/(\bar{d} - d_d)$). Pulse pressures thus obtained were only 1.6 mmHg lower than invasively assessed ones, despite the assumed linear relation between pressure and diameter (van Bortel et al. 2001). However, strong evidence exists for an exponential relationship between arterial cross-section and pressure (van Loon et al. 1977; Hayashi et al. 1980; Stettler et al. 1981; Powałowski and Peńsko 1988). Analysis of the performance of proposed exponential relationships showed correlation coefficients ranging from 0.961 to 0.997 (Powałowski and Peńsko 1988). Given these exponential relationships and assuming that end diastolic and mean arterial pressure do not change over the arterial tree, the pressure diameter relationship can be derived by iteratively changing only a single parameter (*i.e.*, the arterial wall rigidity α) (Powałowski and Peńsko 1988).

It is the aim of this paper to develop a robust method to derive the pressure waveform from the assessed diameter waveform by combining the diameter-derived pulse pressure method (van Bortel et al. 2001) and the exponential relationship between arterial cross-section and pressure (Powałowski and Peńsko 1988). To evaluate the performance of the proposed method, the diameter waveform was assessed in the common carotid artery (CCA) of 51 healthy subjects ranging in age from 22 to 75 years old. From the derived CCA pressure waveforms, the systolic blood pressures were extracted and, together with the estimated pulse pressures, related to the corresponding pressures measured in the brachial artery. Furthermore, continuous incremental elastic modulus, distensibility, compliance and pulse wave velocity will be derived as function of the distending pressure over the cardiac cycle.

MATERIALS AND METHODS

Data acquisition

Using a 7.5-MHz linear-array transducer and fast B-mode, the wall movement of an arterial segment of 15.86 mm was assessed at 16 adjacent positions simultaneously (Meinders and Hoeks 2000; Meinders et al. 2001). Briefly, the frame rate of an echo system (Pie Medical 350, Maastricht, the Netherlands) was increased to 651 Hz by increasing the pulse-repetition frequency (PRF) from 6944 to 10,416 Hz, by increasing the interspacing between echo lines with a factor of four and by reducing the length of the transducer from its original value of 128 to 64 echo lines. Combination of the latter two methods reduced the number of echo lines per frame to 16; hence, increasing the number of frames/s to 651. The envelope of the 16 resulting radiofrequency (RF) lines was displayed on the screen of the US scanner, providing a sparse real-time B-mode image.

Using a specially developed data-acquisition system, the received RF data of each line was digitized with 12-bit resolution and stored on the hard disk of a PC. The RF signals were sampled at 21.3 MHz in accordance with at least twice the received center frequency plus bandwidth (Brands et al. 1997). During off-line postprocessing, first the adventitia-media interface of the anterior wall and the media-adventitia interface of the posterior wall were identified using a sustain attack filter in the first B-mode image after detection of the R-top of the electrocardiogram (ECG) (Hoeks et al. 1995; Meinders et al. 2001), providing the baseline diameter. Thereafter, wall movement was assessed by cross-correlation of subsequently recorded RF lines, resulting in high precision wall tracking (Brands et al. 1997, 1999). Finally, the diameter waveform, *d(t)*, was obtained after averaging over all 16 positions. Similarly, arterial wall thickness was obtained by placing tracking windows at the lumen-intima and media-adventitia interface of the posterior wall (Meinders et al., 2003).

Pressure waveform and arterial wall properties

Arterial cross-section as function of time, *A(t)*, was obtained from the diameter waveform, *d(t)*, according to:

$$A(t) = \frac{\pi d^2(t)}{4}, \tag{1}$$

in which it is assumed that the artery is rotationally symmetrical. The maximum arterial cross-section between two ECG triggers defines the peak systolic arterial cross-section, A_s, whereas the minimum in *A(t)* between the first ECG trigger and A_s defines the end diastolic arterial cross-section, A_d.

The functional relationship between the blood pressure waveform, *p(t)*, and *A(t)* can be expressed as:

$$p(t) = p_0 e^{\gamma A(t)}, \tag{2}$$

in which p_0 and γ are constants (Powałowski and Peńsko

1988). Substitution of *p(t)* and *A(t)* by the end diastolic blood pressure, p_d, and arterial cross-section, A_d, and by the systolic blood pressure, p_s, and arterial cross-section, A_s and solving for p_0 and γ, results in:

$$p(t) = p_d\, e^{\alpha\left(\frac{A(t)}{A_d}-1\right)}, \tag{3}$$

with

$$\alpha = \frac{A_d \ln(p_s/p_d)}{A_s - A_d}. \tag{4}$$

Because eqn (3) is valid over a large pressure range (van Loon et al. 1977; Hayashi et al. 1980; Stettler et al. 1981; Powałowski and Peńsko 1988), the wall rigidity coefficient, α, is pressure-independent (*i.e.*, it does not matter over what pressure range α is determined).

To reconstruct the pressure wave using eqns (3) and (4), p_d and p_s must be obtained simultaneously at the same position as *A(t)*. If the pressure is unknown at the site of arterial cross-section assessment, α cannot be determined directly. However, assuming that p_d and $\bar{p}$ do not change significantly throughout the arterial tree (Nichols and O'Rourke 1998), the pressure wave can be reconstructed. In the process, the mean arterial pressure estimated from *p(t)* in, for example, the CCA is made equal to the mean arterial pressure obtained in, for example, the brachial artery (BrA), by changing iteratively the initial guess of the coefficient α in eqn (3).

As an initial guess for α, A_d and A_s were determined from the measured *A(t)*, whereas p_d and p_s were obtained from standard pressure measurements. For instance, assessing *A(t)* in CCA and p_d and $\bar{p}$ in BrA results in an α of:

$$\alpha = \frac{A_{d,CCA} \ln(P_{s,BrA}/P_{d,BrA})}{A_{s,CCA} - A_{d,CCA}}. \tag{5}$$

Subsequently, $p_{CCA}(t)$ in the common carotid artery was determined according to eqn (3). If $\bar{p}_{CCA}$ is significantly different from $\bar{p}_{BrA}$, α is changed according to:

$$\alpha = \frac{\bar{p}_{BrA}}{\bar{p}_{CCA}}\alpha. \tag{6}$$

Thereafter, $p_{CCA}(t)$ and $\bar{p}_{CCA}$ were again estimated. The iteration stopped if the absolute difference between $\bar{p}_{BrA}$ and $\bar{p}_{CCA}$ was smaller than 0.01 mmHg.

After obtaining *d(t)*, *A(t)* and *p(t)*, not only the diameter, *d(p)*, and arterial cross-section, *A(p)*, can be derived as function of the distending pressure but, also, the incremental elastic modulus, *E(p)*, compliance, *C(p)*, distensibility, *D(p)*, and pulse wave velocity, *PWV(p)*, according to Nichols and O'Rourke (1998):

$$E(p) = \frac{d^2(p)}{2h_{(p)}\dfrac{\delta d(p)}{\delta p}} \tag{7}$$

$$C(p) = \frac{\partial A(p)}{\partial p} \tag{8}$$

$$D(p) = \frac{1}{A(p)} * \frac{\partial A(p)}{\partial p} \tag{9}$$

and

$$PWV(p) = \sqrt{\frac{1}{\rho D(p)}} \approx \sqrt{\frac{1}{\rho\dfrac{1}{A(p)} * \dfrac{\delta A(p)}{\partial p}}}, \tag{10}$$

in which *h(p)* is the arterial wall thickness at pressure *p*, ρ the density of blood (10^3 kg/m^3), $\partial d(p)/\partial p$ and $\partial A(p)/\partial p$ the partial derivatives of diameter and arterial cross-section with respect to pressure. Equations (7)–(10) determine arterial wall properties as function of the distending pressure, contrary to the usual assessment of *E*, *D*, *C* and *PWV* using the diastolic-systolic pulse pressure:

$$E = \frac{d_d^2}{h\dfrac{\Delta d}{\Delta p}}, \tag{11}$$

$$C = \frac{\Delta A}{\Delta p}, \tag{12}$$

$$D = \frac{\Delta A}{A_d \Delta p} \tag{13}$$

and

$$PWV = \frac{1}{\sqrt{\rho D}}, \tag{14}$$

with Δp as the pulse pressure ($p_s - p_d$), Δd the pulse diameter ($d_s - d_p$) and ΔA the pulse cross-sectional area ($A_s - A_d$).

Study subjects

Validation of the proposed method was performed through an *in vivo* study in 51 (20 men, 31 women) presumably healthy volunteers ranging in age from 21 to 75 years old (mean 50 ± 14 years). All subjects gave written informed consent to participate in the study, which was approved by the joint medical ethical committee of the Academic Hospital Maastricht and the Maastricht University. The site of measurement was a longitudinal section of the left CCA with the most distal RF line 2 to 3 cm proximal to the bifurcation and the scan plane perpendicular to the plane of the bifurcation as established with the echo system. The method is evaluated in the CCA because it is easily assessable and prone to changes in arterial wall properties such as atherosclerosis. The depth window size for the correlation procedure was set to the resolution of the system (*i.e.*, 0.3 mm), equivalent to 8 sample points at a sampling frequency of 21.3 MHz. The temporal window size was set to 7 frames, converting to a temporal resolution of 10 ms at a frame rate of 651 Hz (Brands et al. 1997, 1999; Meinders et al. 2001).

In each subject, six independent measurements were made during one session. The recording time of each measurement was 6 s, covering at least five cardiac cycles (intersubject average 6.4). During measurements, subjects were not allowed to move, swallow or cough. Before the start of each measurement, the position of the transducer was optimized. The time between each measurement was about 1 to 2 min. An ECG was recorded simultaneously with the B-mode measurement. The pulse pressure was determined before, between and after measurements in the left brachial artery using an oscillometric blood pressure meter (Omron 705CP). Mean arterial pressure was obtained from $\bar{p} = p_d + (p_s - p_d)/3$. Values presented in the Results section are averages and SD over all measurements.

RESULTS

Figure 1 shows the pressure waveforms (thick lines), derived from the change in arterial cross-sections (thin lines) in the left CCA for (top) a young and (bottom) an older subject. For each beat, we determined the arterial diameter. Due to the precision of the diameter detection procedure, end diastolic arterial cross-section changes from beat to beat, explaining the sudden changes in the arterial cross-section waveform. However, the pressure wave itself is independent of these small changes in cross-section because only the shape of the change in cross-section during the cardiac cycle was used. The change in arterial cross-section in the older subject is much smaller than in the younger subject, whereas the pulse pressure is much higher, a feature also expressed in

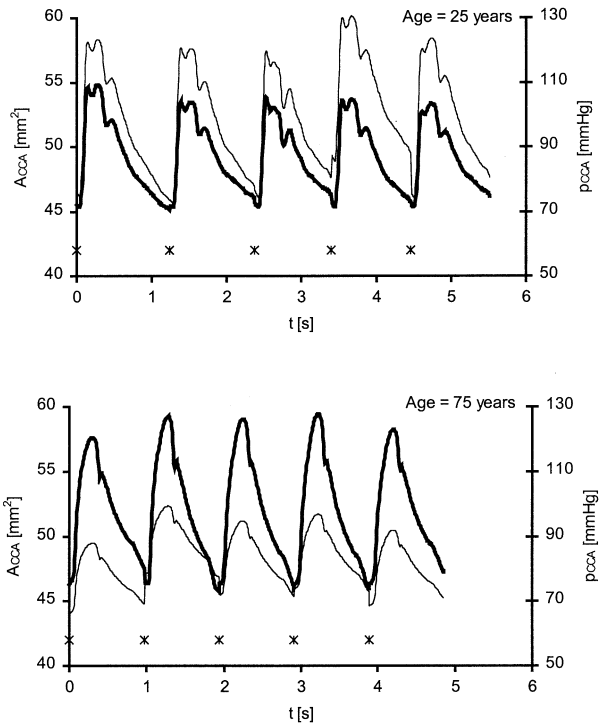

Fig. 1. Pressure waveform (thick line) as estimated from the arterial cross-sectional change (thin line) in (top) a young and (bottom) old subject as function of time. The ECG triggers are indicated by *.

the rate of increase in arterial cross-section as function of estimated blood pressure in CCA (Fig. 2). The decreased slope of the older subject (thin lines) indicates larger wall rigidity ($\alpha = 4.4$) (*i.e.*, stiffer arteries) in comparison to that in the younger subject ($\alpha = 1.6$; thick lines). The logarithmic increase in arterial cross-section as function of distending pressure is a result of the fitting procedure,

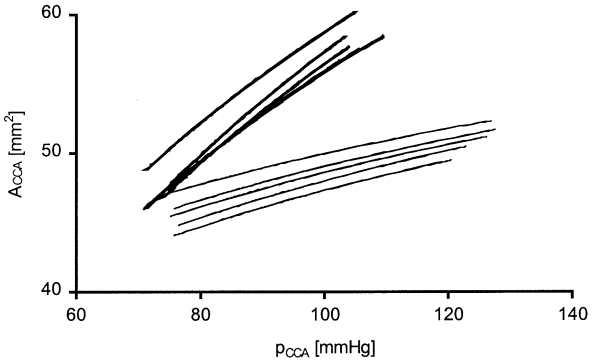

Fig. 2. Arterial cross-section as function of arterial pressure for (thick lines) a young and (thin line) old subject. Each line represents one complete beat.

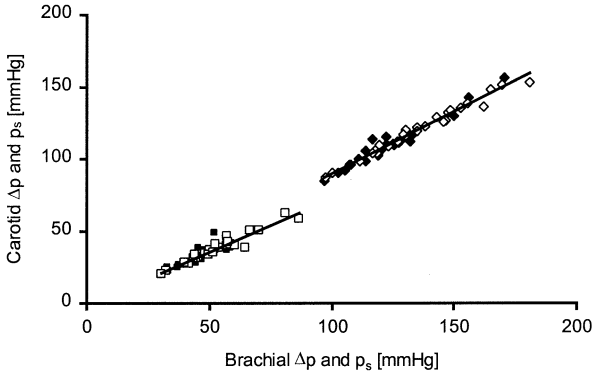

Fig. 3. Pulse pressure, Δp (♦), and peak systolic pressure, p_s (□), in the common carotid artery plotted against Δp and p_s in the brachial artery. Solid markers indicate subjects younger than 50 years old, open markers indicate subjects more than 50 years old. (—) linear least square fits (*i.e.*, $\Delta p_{CCA} = 0.71 * \Delta p_{BrA}$ (correlation coefficient = 0.94) and $p_{s,CCA} = 0.88 * p_{s,BrA}$ (correlation coefficient = 0.98).

as described in the Materials and Methods section, eqns (3) and (4).

The peak systolic and pulse pressures in the CCA are plotted in Fig. 3 as function of the brachial peak systolic and pulse pressure for young subjects and older subjects. The solid lines indicate linear least square fits with slopes of 0.88 and 0.71 and correlation coefficients of 0.98 and 0.94 for peak systolic and pulse pressures, respectively. That is, in CCA, systolic pressures are 12% lower than BrA systolic pressures, whereas CCA pulse pressures are 29% lower than BrA pulse pressure.

The arterial wall rigidity, α, increases with age, indicating stiffer arteries at higher ages (Fig. 4). A linear least square fit between α and age results in a regression line ($\alpha = 0.421 + 0.0602 *$ age, correlation coefficient = 0.76), comparing well to the regression line ($\alpha = 0.858 + 0.0523 *$ age) found by Powałowski and Peńsko (1988).

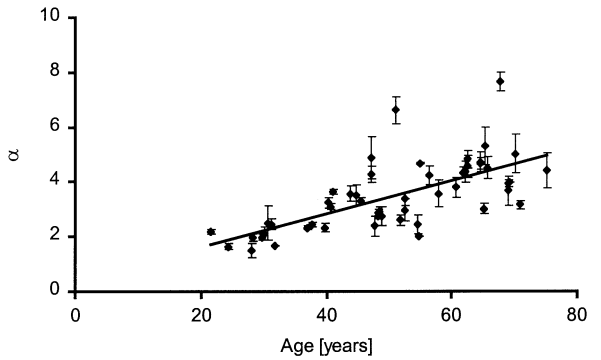

Fig. 4. The increasing arterial wall rigidity, α, as function of age, indicates stiffer arterial walls at higher ages. Error bars are the intrasubject SDs over six consecutive recorded measurements. (—) = linear least square fit between α and age ($\alpha = 0.421 + 0.0602 *$ age, correlation coefficient = 0.76).

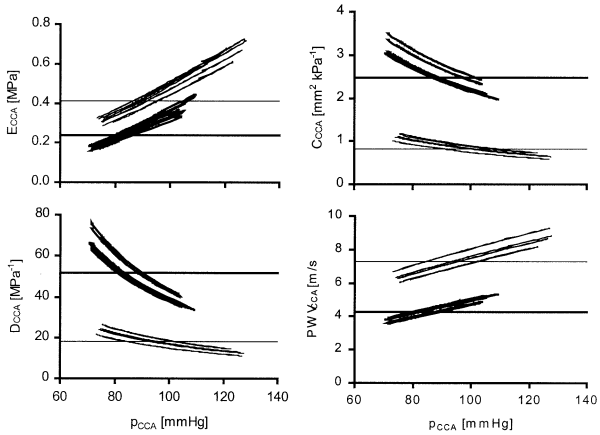

Fig. 5. (top left)E = incremental elastic modulus; (top right) C = compliance; (bottom left) D = distensibility, and (bottom right) PWV = pulse wave velocity as function of pressure (five consecutive heart beats) for a young subject (age = 25 years old, thick lines) and an old subject (age = 75 years old, thin lines) in the CCA. The horizontal lines indicate arterial wall properties assessed over the complete diastolic-systolic pressure range, eqn (11).

The nonlinear relation between distending pressure and incremental elastic modulus, *E(p)*, distensibility, *D(p)*, compliance, *C(p)* and pulse wave velocity, *PWV(p)*, as derived from eqns (7)–(10), are shown in Fig. 5 over five consecutive heart cycles for a young subject (age = 25 years old) and older subject (age = 75 years old). Due to the pressure-dependence of arterial wall properties, *E*, *C*, *D* and *PWV* change during the cardiac cycle (Fig. 6). For comparison, we have also indicated arterial wall properties assessed using the conventional approach, as given in eqn (11).

Results are summarized in Table 1 for each decade, together with the average intrasubject SDs. Pressures and SDs obtained in the brachial artery were based on three oscillometric measurements. The relative small intrasubject SD as compared to the range of pressures investigated (Fig. 3) is a result of the precision to assess pressure and the change in pressure during the measurements. Because carotid p_d and $\bar{p}$ were set to brachial artery pressures, they are not displayed. Carotid p_s and Δp were derived from the cross-sectional change, resulting in much lower intrasubject SDs, because the diameter waveform could be assessed with a high precision of about 30 μm and the average over 16 adjacent lines was considered (Hoeks et al. 1999; Meinders and Hoeks 2000).

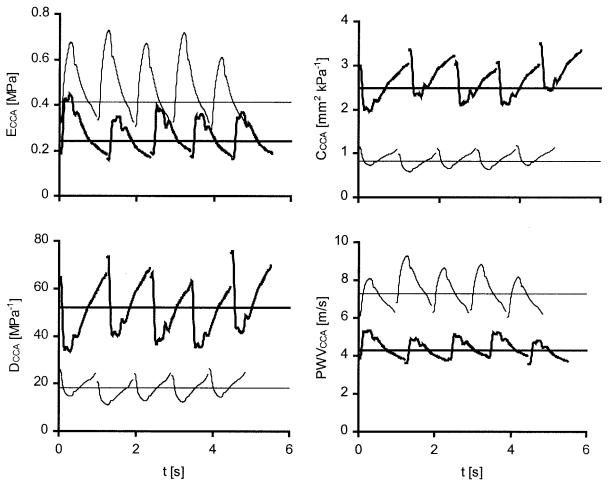

Fig. 6. (top left) E = incremental elastic modulus, (top right) C = compliance, (bottom left) D = distensibility and (bottom right) PWV = pulse wave velocity. As a function of time (consecutive heart beats) of a young subject (age = 25 y, thick lines) and an old subject (age = 75 y, thin lines) in the common carotod artery (CCA). The horizontal lines indicate arterial wall properties assessed over the complete diastolic-systolic pressure range, eqn (11).

DISCUSSION

In this study, the blood pressure waveform was estimated from the arterial change in cross-section in arteries of which the diameter waveform can be determined easily with US. To this end, the arterial cross-section during the cardiac cycle was related to the pressure and wall rigidity using an empirically derived exponential relationship and end diastolic and mean arterial pressure as calibrating values. After the arterial cross-section and pressure waveforms are known, compliance, distensibility, pulse wave velocity and elastic modulus can be derived as function of the distending pressure. The proposed method was applied to the left common carotid artery.

There are several crucial transformations in the conversion of diameter to pressure. The transformation from diameter to arterial cross-section assumes that arteries are rotationally symmetrical due to the high transmural pressure, a feature that has been generally accepted (Nichols and O'Rourke 1998). The transformation from arterial cross-section to pressure using the empirically derived exponential relationship has been the subject of research by many authors (van Loon et al. 1977; Hayashi et al. 1980; Stettler et al. 1981; Powałowski and Peńsko 1988). Powałowski and Peńsko (1988) showed high correlation coefficients between experimental data obtained in the common carotid artery and the proposed functions. Hayashi et al. (1980) showed that the exponential relationship is not only valid in the common carotid artery but, also, in femoral, internal carotid, intracranial and extracranial vertebral arteries. The calibration procedure is based on the observation that p_d and $\bar{p}$ are reasonably constant throughout the major peripheral arteries (Nichols and O'Rourke 1998). For instance, Pauca et al. (1992) showed that the difference between p_d and $\bar{p}$ was only 0.2 mmHg larger in the radial artery than in the ascending aorta.

The exponential relationship between pressure and diameter assumes negligible viscoelastic properties of arteries. Although viscoelastic properties have been reported (Boutouyrie et al. 1997; Shau et al. 1999), methods to assess viscoelastic properties suffer, not only from the spatial separation of two different transducers but, also, from different signal-processing procedures, resulting in ill-defined pressure-diameter relationships due to the phase delays introduced between both signals (Hoeks et al. 2000). Furthermore, part of the reported decrease in mean arterial pressure of 1 mmHg over the arterial tree (Pauca et al. 1992) can be accounted for by the shear stress exerted by the blood flow on the arterial wall (Fung 1984). Hence, the effect of viscoelastic properties on the change in pressure and diameter-pressure relationship is believed to be small.

Table 1. Common carotid and brachial artery properties together with the average intrasubject SDs subdivided in decades

		Brachial artery				Common carotid artery		
Age (years)	n	p_d (mmHg)	$\bar{p}$ (mmHg)	p_s (mmHg)	Δp (mmHg)	p_s (mmHg)	Δp (mmHg)	α
20–30	6	72 ± 4	85 ± 3	113 ± 6	41 ± 7	102 ± 1	34 ± 4	1.9 ± 0.2
30–40	6	74 ± 3	89 ± 3	120 ± 5	47 ± 6	106 ± 4	28 ± 5	2.3 ± 0.3
40–50	13	82 ± 3	97 ± 3	129 ± 7	47 ± 8	115 ± 1	31 ± 3	3.3 ± 0.3
50–60	9	80 ± 4	95 ± 3	125 ± 7	45 ± 7	112 ± 2	32 ± 4	3.6 ± 0.3
60–70	14	84 ± 5	104 ± 4	142 ± 7	58 ± 8	126 ± 2	33 ± 5	4.5 ± 0.4
70–80	3	83 ± 3	103 ± 4	143 ± 8	60 ± 8	126 ± 2	36 ± 4	4.2 ± 0.5

p_d = end diastolic pressure; p_s = peak systolic pressure; $\bar{p}$ = mean arterial pressure; Δp = pulse pressure; α = wall rigidity.

Validation of blood pressures estimated for the CCA is difficult due to the limited data published. Available data is usually obtained during catheterization of subjects suffering from coronary heart disease compromising the blood pressure. However, even in these patients, the ratios of carotid and brachial pressures are comparable to the healthy subjects in this study. For instance, Kelly and Fitchett (1992) performed invasive pressure readings in the aortic arch and brachial artery during cardiac catheterization of patients with angina pectoris due to significant coronary artery stenosis. Although patients had high pulse pressures (61 mmHg) and low end diastolic pressures (66 mmHg), possibly due to the antianginal medication given, the ratio of Δp in carotid and brachial artery was on the order of 0.75, whereas the ratio of peak systolic pressures was $\approx$ 0.92, comparing reasonably well to our results (0.71 and 0.88, respectively) (Fig. 3). The slightly higher ratios in patients with coronary artery stenosis are also seen in patients with end-stage renal disease, where pressure ratios increase up to 1 for the highest score of arterial calcification (Blacher et al. 2001).

Assuming the same p_d and $\bar{p}$ throughout the main arteries provides, after iteration, the wall rigidity coefficient α. The obtained α is the wall rigidity at the site of arterial cross-section assessment and does not depend on pressure because the exponential relationship is valid over a large pressure range (van Loon et al. 1977; Hayashi et al. 1980; Stettler et al. 1981; Powałowski and Peńsko 1988). Hence, high values of α must result from local structural changes in the arterial wall. The two subjects with a relatively high α do, indeed, have a low relative change in arterial cross-section ($\approx$ 5%) despite normal end diastolic (73 mmHg) and peak systolic pressures (104 mmHg) in the CCA. Only A_d differs between the two subjects (34 and 50 mm^2), but is not significantly different from others in the group. Estimating α by inserting brachial p_d and p_s in eqn (4) results in a wall rigidity that is too low, explaining the lower values of α found by Powałowski and Peńsko (1988) in healthy subjects.

The precision of the method to determine Δp and p_s in CCA is high and depends only on the precision to determine distension in CCA ($\approx$ 30 μm) and p_d and $\bar{p}$ in BrA (Table 1). The mean arterial pressure has been calculated using $\bar{p} = p_d + (p_s - p_d)/3$, which has been shown to be valid in large population studies, but is possibly inaccurate in individuals. Real-time assessment of the diastolic and mean pressures in, for example, the radial artery using applanation tonometry or in the finger (digital artery) using photoplethysmography, will improve the results. The obtained pressures are independent of the baseline end diastolic diameter, as can be seen from eqns (3) and (4),(*i.e.*, using the internal instead of external arterial diameter will result in a larger relative change in arterial cross-section, but lowers α while p_d, p_s and $\bar{p}$ remain unchanged). The fact that wall rigidity depends on the precision to determine the initial wall position ($\approx$ 100 μm) explains the relatively high SDs in α ($\approx$ 10%).

To our knowledge, this is the first time that *E*, *C*, *D* and *PWV* have been simultaneously assessed as function of the distending pressure (Fig. 5). Moreover, deriving the pressure waveform from the diameter waveform ensures zero phase delay due to spatial separation and different signal processing of two separate transducers. The increase in incremental *E* and *PWV* and decrease in incremental *C* and *D* as function of increasing blood pressure is a result of arteries becoming stiffer at higher distending pressures. During the cardiac cycle, pressure in arteries is pulsatile (Fig. 1), explaining the change in *E*, *PWV*, *C* and *D* as function of time (Fig. 6). The relatively larger change in arterial properties during the cardiac cycle has also been observed by other authors (Bussy et al. 2000). The nonlinear relation shown in Figs. 5 and 6 is also the reason for the large variation in published arterial wall properties. For instance, determining *PWV* using the foot-to-foot method results in a *PWV* at diastolic pressures (Chiu et al. 1991), whereas determining *PWV* using the Bramwell-Hill equation, eqn (11), results in a *PWV* at a larger distending pressure (*i.e.*, approximately the mean systemic pressure) (Figs. 5 and 6) Moreover, intersubject comparison of arterial wall properties based on eqn (11) is questionable because the actual pressure is unknown and changes with the property analyzed (*i.e.*, the position of the intersection between the nonlinear relation and the horizontal lines in Fig. 5 are not the same for *E*, *D*, *C* and *PWV*).

Proper intersubject comparison of arterial wall properties should be done at the same distending pressure. This isobaric comparison can lead to surprising results. For instance, isobaric determination of the elastic modulus in hypertensive and nonhypertensive subjects showed no significant difference between these two groups (Bussy et al. 2000). The method presented here results, not only in a functional relationship between arterial wall properties and distending pressure, but, also, allows selection of isobaric values to facilitate proper intersubject comparison of arterial wall properties.

CONCLUSIONS

Pressure waveforms can be derived from arterial cross-sections by iteratively calibrating an exponential relationship between pressure and arterial cross-section to end diastolic and mean arterial pressure. Because both signals underwent identical signal processing, and due to the absence of spatial separation between the two signals,

there was no phase delay, enabling proper evaluation of incremental compliance, distensibility, pulse wave velocity and elastic modulus. The proposed method uses only one transducer, is noninvasive, is simple to implement and results in an estimate of the wall rigidity. In healthy subjects, the carotid pulse and mean arterial pressure are 29% and 12% lower than brachial artery pulse and mean pressures, respectively. After the pressure waveform is derived from the diameter waveform, other local arterial parameters such as pulse-wave velocity, incremental elastic modulus, distensibility and compliance can be derived as function of the distending pressure during the cardiac cycle, providing the possibility of isobaric comparison of arterial wall properties between subjects. Although, in this study, the method was applied to CCA, it can be applied to any artery in the arterial tree.

Acknowledgments—Dr. Jan M. Meinders was supported by a grant (BTS97126) from SENTER, Ministry of Economic Affairs, the Netherlands.

REFERENCES

Blacher J, Guerin AP, Pannier B, Marchais SJ, London GM. Arterial calcifications, arterial stiffness, and cardiovascular risk in end-stage renal disease. Hypertension 2001;38:938–942.

Boutouyrie P, Bezie Y, Lacolley P, et al. In vivo/in vitro comparison of rat abdominal aorta wall viscosity. Influence of endothelial function. Arterioscler Thromb Vasc Biol 1997;17:1346–55.

Brands PJ, Hoeks AP, Ledoux LA, Reneman RS. A radiofrequency domain complex cross-correlation model to estimate blood flow velocity and tissue motion by means of ultrasound. Ultrasound Med Biol 1997;23:911–920.

Brands PJ, Hoeks AP, Willigers J, Willekes C, Reneman RS. An integrated system for the non-invasive assessment of vessel wall and hemodynamic properties of large arteries by means of ultrasound. Eur J Ultrasound 1999;9:257–266.

Bussy C, Boutouyrie P, Lacolley P, Challande P, Laurent S. Intrinsic stiffness of the carotid arterial wall material in essential hypertensives. Hypertension 2000;35:1049–1054.

Chiu YC, Arand PW, Shroff SG, Feldman T, Carroll JD. Determination of pulse wave velocities with computerized algorithms. Am Heart J 1991;121:1460–1470.

Fung YC. Biodynamics circulation. New York Berlin Heidelberg Tokyo: Springer-Verlag New York, Inc., 1984.

Hayashi K, Handa H, Nagasawa S, Okumura A, Moritake K. Stiffness and elastic behavior of human intracranial and extracranial arteries. J Biomech 1980;13:175–184.

Hoeks AP, Brands PJ, Smeets FA, Reneman RS. Assessment of the distensibility of superficial arteries. Ultrasound Med Biol 1990;16: 121–128.

Hoeks AP, Brands PJ, Willigers JM, Reneman RS. Non-invasive measurement of mechanical properties of arteries in health and disease. Proc Inst Mech Eng 1999;213(part H):195–202.

Hoeks AP, Willekes C, Boutouyrie P, et al. Automated detection of local artery wall thickness based on M-line signal processing. Ultrasound Med Biol 1997;23:1017–1023.

Hoeks AP, Willigers JM, Reneman RS. Effects of assessment and processing techniques on the shape of arterial pressure-distension loops. J Vasc Res 2000;37:494–500.

Hoeks APG, Di X, Brands PJ, Reneman RS. An effective algorithm for measuring diastolic artery diameters. In: Filipczynski L, Nowicki A, eds. ICB seminars on biomeasurements: Ultrasound in biomeasurements, diagnostic and therapy. Warsaw: ICB, 1995:68–79.

Kelly R, Fitchett D. Noninvasive determination of aortic input impedance and external left ventricular power output: A validation and repeatability study of a new technique. J Am Coll Cardiol 1992; 20:952–963.

Meinders JM, Hoeks APG. 2-D detection of vessel wall inhomogeneities. 9th Congress of World Federation for Ultrasound in Medicine and Biology. Ultrasound Med Biol 2000;26:A94.

Meinders JM, Brands PJ, Willigers JM, Kornet L, Hoeks AP. Assessment of the spatial homogeneity of artery dimension parameters with high frame rate 2-D B-mode. Ultrasound Med Biol 2001;27: 785–794.

Meinders JM, Kornet L, Hoeks AP. Assessment of spatial inhomogeneities in intima media thickness along an arterial segment using its dynamic behavior. Am J Physiol Heart Circ Physiol 2003;285: H384–391.

Millasseau SC, Guigui FG, Kelly RP, et al. Noninvasive assessment of the digital volume pulse. Comparison with the peripheral pressure pulse. Hypertension 2000;36:952–956.

Nichols WN, O'Rourke MF. McDonald's blood flow in arteries. London: Edward Arnold, 1998.

O'Rourke MF. Mechanical principles. Arterial stiffness and wave reflection. Pathol Biol (Paris) 1999;47:623–633.

Pauca AL, Wallenhaupt SL, Kon ND, Tucker WY. Does radial artery pressure accurately reflect aortic pressure? Chest 1992;102:1193–1198.

Powałowski T, Peńsko B. A noninvasive ultrasonic method for the elasticity evaluation of the carotid arteries and its application in the diagnosis of the cerebro-vascular system. Arch Acoust 1988;13: 109–126.

Segers P, Carlier S, Pasquet A, et al. Individualizing the aorto-radial pressure transfer function: Feasibility of a model-based approach. Am J Physiol Heart Circ Physiol 2000;279:H542–H549.

Shau YW, Wang CL, Shieh JY, Hsu TC. Noninvasive assessment of the viscoelasticity of peripheral arteries. Ultrasound Med Biol 1999;25:1377–1388.

Stettler JC, Niederer P, Anliker M. Theoretical analysis of arterial hemodynamics including the influence of bifurcations. Part I: Mathematical models and prediction of normal pulse patterns. Ann Biomed Eng 1981;9:145–164.

van Bortel LM, Balkestein EJ, van der Heijden-Spek JJ, et al. Noninvasive assessment of local arterial pulse pressure: Comparison of applanation tonometry and echo-tracking. J Hypertens 2001;19: 1037–1044.

van Loon P, Klip W, Bradley EL. Length-force and volume-pressure relationships of arteries. Biorheology 1977;14:181–201.